Chem Biol Drug Des 2016; **87:** 382–397

Research Article

Hemisynthesis, Antitumoral Effect, and Molecular Docking Studies of Ferutinin and Its Analogues

Rémi Safi[1,2], Fréderic Rodriguez[2], Georges Hilal[3], Mona Diab-Assaf[1], Youssef Diab[1], Marwan El-Sabban[4], Fadia Najjar[1,*] and Evelyne Delfourne[2,*]

[1]Department of Chemistry and Biochemistry, Faculty of Sciences II/EDST, Lebanese University, Jdeidet el Metn - Fanar, Lebanon
[2]Laboratoire de Synthèse et Physicochimie des Molécules d'Intérêt Biologique, UMR CNRS 5068, Université Paul Sabatier, 118 route de Narbonne, 31062 Toulouse Cédex, France
[3]Cancer and Metabolism Research Laboratory, Faculty of Medicine, Saint Joseph University, Beirut, Lebanon
[4]Department of Anatomy, Cell Biology and Physiological Sciences, Faculty of Medicine, American University of Beirut, Beirut, Lebanon
[*]Corresponding authors: Fadia Najjar, fadia.najjar@gmail.com and Evelyne Delfourne, delfourn@chimie.ups-tlse.fr

The natural product ferutinin was shown to act as an agonist to estrogen receptor ERα and agonist/antagonist to ERβ featuring a weak antiproliferative activity toward breast cancer cells. To enhance this activity, ferutinin analogues were synthesized by esterification of jaeschkenadiol with different acids. These compounds were assayed for their *in vitro* antiproliferative activity against estrogen-dependent (MCF-7) and estrogen-independent (MDA-MB-231) breast cancer cell lines. Among the compounds, 3c' exhibited a potent inhibitory selective activity against MCF-7 with IC_{50} value of 1 μM. Docking simulation of 3c' in the ligand binding domain of the ERs indicated a potential antagonism interaction with both ER subtypes. Functional assay showed that 3c' binds as an antagonist to ERα protein while ferutinin acts as an agonist.

Key words: antitumor agents, breast cancer, estrogen receptors, *Ferula hermonis*, ferutinin, jaeschkenadiol, molecular docking

Received 5 July 2015, revised 7 September 2015 and accepted for publication 10 September 2015

Uncontrolled proliferation in breast cancer cells is dependent upon estrogen and related processes. Therefore, an effective strategy in estrogen-dependent cancer treatment has been proven to interfere with hormonal status in order to halt the proliferation and to induce apoptosis in tumor cells. Estrogens exert their effect by binding to their receptors (ERα and ERβ) and thus by activating the survival transcription machinery. Recently, much attention has been focused on natural phytoestrogens as potent antagonist to ER, especially in the case of breast cancer, which is the most common cause of cancer-related deaths among women (1,2).

Ferula species are good sources of biologically active compounds such as terpenoid coumarins and sesquiterpene derivatives (3,4). These species are documented in the traditional medicine of the Middle East area and have been particularly used for their potent chemopreventive cancer activities.

Ferutinin, the main component of *Ferula hermonis* (5), an endemic plant of Syria and Lebanon, is a *p*-hydroxybenzoyl ester of jaeschkenadiol, which exhibits a broad spectrum of activities (6–11). This molecule is a potent phytoestrogen, with high affinity for both ER subtypes (ERα: IC_{50} = 33.1 nM and ERβ: 180.5 nM, in competitive binding assays) (12). It can bind to both ERs, acting as an agonist for ERα and as an agonist/antagonist for ERβ (12) for which it is thus considered as a selective estrogen receptor modulator (SERM) (13).

Ferutinin cancer preventing properties have been increasingly investigated because this daucane sesquiterpene has proven to be cytotoxic against several cancer cells. The antiproliferative effect of ferutinin was previously reported on both estrogen-dependent (14,15) and estrogen-independent cell lines (15–17). An interesting biphasic effect was observed on the proliferation of estrogen-dependent breast cancer cell line MCF-7, when treated with increasing concentrations of ferutinin. At lower concentrations of the drug, a proliferative effect was observed, whereas an antiproliferative effect was shown at higher concentrations (14). Previous structure-activity investigations on ferutinin have shown that the daucane core containing the double bond (C8/C9) and the C6 configuration were crucial for the cytotoxic activity of the molecule and that the binding of ferutinin to ERs was possible through the *p*-hydroxybenzoyl moiety (13).

On the basis of these results as well as on our interest in the development of new anticancer agents issued from

 doi: 10.1111/cbdd.12670

Lebanese plants, we describe herein the hemisynthesis and *in vitro* antiproliferative activity of three series of ferutinin analogues (Figure 1).

Methods and Materials

Chemistry

General

Infrared spectra were recorded on a Perkin-Elmer FT-IR 1725X instrument. ^{1}H NMR spectra were recorded with a Bruker Advance 300 MHz and advance 500 MHz spectrometer (300 and 500 MHz, respectively), using TMS as an internal standard. Chemical shifts were referenced to the residual solvent signal (CDCl3, delta 7.27). MS spectra were recorded on a ThermoQuest TSQ 7000 (San Jose, CA, USA) or a ThermoFinnigan MAT 95 XL (Bermen, Germany) for HRMS spectrum. All compounds were routinely checked by TLC and ^{1}H NMR. TLCs were performed on Merck silica gel 60F254 and visualized under light at 254 nm or with phosphomolybdic acid revelation. Silica gel (15–40 μm, E. Merck, Kenilworth, NJ, USA) was used for column chromatography. After extractions and reactions, solvent was removed using rotary evaporator under reduced pressure. Organic solutions were dried over anhydrous magnesium sulfate.

Plant material

A sample of *Ferula hermonis* roots collected on Mount Hermon was purchased in May 2010 in Beirut and identified by Pr Samir SAFI from the Lebanese University, faculty of Sciences. A voucher specimen is deposited at herbanium at the faculty of Sciences, Lebanese University.

Extraction and isolation of jaeschkenadiol

Air-dried and coarsely powdered roots of Ferula hermonis (17 g) were extracted with CH_2Cl_2 (250 mL) in a soxhlet apparatus. Concentration of the extracts, at room temperature under reduced pressure, provided viscous oil (4.5 g, 26.5%).

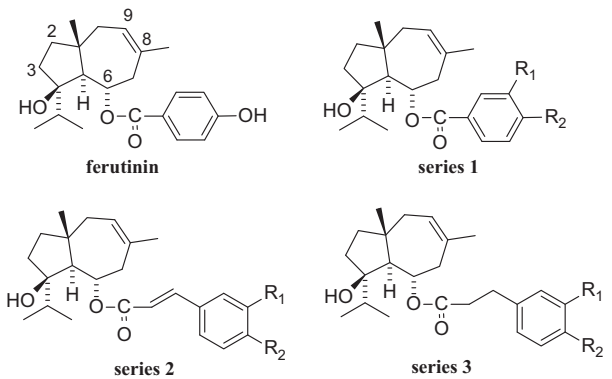

Figure 1: Ferutinin and its analogues.

One gram of this oil was refluxed with 10% KOH (50 mL) methanol solution. After 1 h, thin layer chromatography analysis (petroleum ether-EtOAc 8/2, jaeschkenadiol Rf: 0.31) showed that the reaction was complete. After cooling, the reaction mixture was acidified with 1 M HCl 100 mL) and extracted with CH_2Cl_2 (100 mL). The combined methylene chloride phases were washed with brine, dried, and evaporated. The mother liquors were purified by chromatography (petroleum ether-ETOAc8/2, jaeschkenadiol Rf = 0.26) to obtain crystalline jaeschkenadiol.

1-isopropyl-3a, 6 dimethyl-1, 2, 3, 3a, 4, 7, 8, 8a-octahydroazulene-1,8-diol (jaeschkenadiol). 470.2 mg, 41% yield, white crystalline powder; IR (cm^{-1}): 3337, 1723, 1663. ^{1}H NMR ($CDCl_3$) δ 5.44 (br s, 1H), 3.91 (td, J = 2.5 Hz and J = 12.5 Hz, 1H), 2.31 (br t, 1H), 2.18 (dd, J1 = 3 Hz and J = 14.5 Hz, 1H), 2.10 (sept, J = 6.5 Hz, 1H), 1.96 (dd, J = 6 Hz and J = 14.5 Hz, 1H), 1.93 (dd, J = 8 Hz and J = 14 Hz, 1H), 1.80–1.83 (m, 1H), 1.76 (s, 3H), 1.66 (d, J = 10.5 Hz, 1H), 1.55 (td, J = 8 Hz and J = 14 Hz, 1H), 1.42 (dd, J = 7.5 Hz and J = 12.5 Hz, 1H), 1.16 (ddd, J = 8.5 Hz and J = 12.5 Hz, 1H), 0.97 (s, 3H), 0.92 (d, J = 7 Hz, 3H), 0.88 (d, J = 7 Hz, 3H); ^{13}C NMR ($CDCl_3$) δ 17.6, 18.6, 20.2, 26.4, δ 31.4, 37.0, 40.9, 41.2, 41.4, 44.1, 60.1, 71.3, 87.1, 125.3, 133.5; DCI-MS (*m/z*): 221.1 (MH^+-H2O). HRMS (DCI) calcd for $C_{15}H_{25}O$: 222.1905, found: 221.1917 (MH^+- H2O).

General procedure for the synthesis of acids 4a, 4b, 4d, 5c, and 5d. Acid (829 mmol) was dissolved under stirring in pyridine (1.15 l), cooling to T <5 °C on an ice bath. The resulting solution was added with 4-dimethylaminopyridine (DMAP, 248.8 mmol) and pivaloyl chloride (2.487 mol). The solution was allowed to warm up to room temperature and left under stirring for 2 h, then added with water (2.29 l) and left under stirring for further 3 h. The solution was poured into a separatory funnel and extracted with CH_2Cl_2 (750 mL). The combined methylene chloride phases were washed with 2 M H_2SO_4 (750 mL) and a saturated NaCl solution (1150 mL), then dried over Na_2SO_4 (60 g). The solution was filtered through paper filter, and the solvent was evaporated off under vacuum to obtain a residue which is triturated with petroleum ether at 30°–50° (400 mL), filtered by suction, and dried under vacuum in a static dryer at 45 °C for 15 h to give the desired product.

4-(1, 1-dimethylethoxy) benzoïc Acid (4a). A suspension of hexane washed sodium hydride (1.3 g of a 60% suspension in oil) in dry dimethylsulfoxide (15 mL) was heated at 70 °C under nitrogen for 1 h. It was then cooled to 30 °C, and 1.5 g of tertiary butanol was slowly added. The resultant mixture was stirred for 30 min, and then, 2.4 g of *para*-fluorobenzonitrile was added, and stirring was continued at room temperature overnight. The reaction mixture was heated at 60 °C for 6 h and then cooled

and diluted with diethyl ether. The ether solution was washed with water and brine and was then dried over sodium sulfate and evaporated to give an oily residue. A total of 3.3 g of the residue is refluxed overnight with 5.0 mL of 2N sodium hydroxide in ethanol (40 mL). The mixture was then concentrated to dryness, re-dissolved in water, and washed with diethyl ether. The aqueous phase was acidified with 2N hydrochloric acid and then extracted with methylene chloride. The organic fractions were combined, dried over sodium sulfate, and then evaporated to give oil, which was chromatographed on silica gel with methylene chloride as the eluent to yield the title compound as a white powder product.

1.16 g, 59% yield, white powder; m.p. l32–133 °C. ^{1}H NMR ($CDCl_3$): δ 8.03 (d, J = 6.9 Hz, 2H), 7.05 (d, J = 6.6 Hz, 2H), 1.43 (s, 9H). DCI-MS (*m/z*): 213.1 (MNH_4^+).

***p*-pivaloyloxybenzoïc acid (4b).** Starting from p-hydroxybenzoic acid (1.15 g, 829 mmol), 4b was obtained (1.28 g, 70% yield, white powder); ^{1}H NMR ($CDCl_3$): δ 8.16 (d, J = 8.7 Hz, 2H), 7.21 (d, J = 8.7 Hz, 2H), 1.41 (s, 9H). DCI-MS (*m/z*): 240.1 (MNH_4^+).

3-methoxy-4-(pivaloyloxy) benzoïc acid (4d). Starting from vanillic acid (140 mg, 829 mmol), 4d was obtained (Quantitative yield, white powder); ^{1}H NMR ($CDCl_3$): δ 7.72 (dd, J = 3 Hz and J = 9 Hz, 1H), 7.66 (d, J = 3 Hz, 1H), 7.08 (d, J = 6 Hz, 1H), 3.86 (s, 3H), 1.37 (s, 9H).

(E)-3-(4-(pivaloyloxy) phenyl) acrylic acid (5c). Starting from coumaric acid (136 mg, 829 mmol), 5c was obtained (182 mg, 88% yield, white powder); ^{1}H NMR ($CDCl_3$): δ 7.75 (d, J = 15 Hz, 1H), 7.56 (d, J = 9 Hz, 2H), 7.10 (d, J = 9 Hz, 2H), 6.4 (d, J = 18 Hz, 1H), 1.36 (s, 9H).

(E)-3-(3-methoxy-4-(pivaloyloxy) phenyl) acrylic acid (5d). Starting from ferulic acid (1.63 g, 829 mmol), 5d was obtained (1.77 g, 77% yield, white powder); ^{1}H NMR ($CDCl_3$): δ 7.77 (d, J = 15.9 Hz, 1H), 7.20 (d, J = 6 Hz, 1H), 7.17 (dd, J = 8.4 Hz and J = 1.8 Hz, 1H), 7.08 (d, J = 8.1 Hz, 1H), 6.43 (d, J = 15 Hz, 1H), 3.89 (s, H15, 3H), 1.41 (s, 9H).

General procedure for the synthesis of acids 5e and 6c. To a solution of acid (1 mmol) in pyridine (2 mL), anhydride acetic (2 mL) was added and left under stirring overnight. The mixture was hydrolyzed using saturated solution of $NaHCO_3$ (3 mL), then extracted with CH_2Cl_2 (3 mL). The methylene chloride phases were washed with water (3 mL), then dried over MgSO4 and evaporated to give the desired acid.

3-(4-acetoxyphenyl) propanoïc acid (5e). Starting from 3-(p-hydroxyphenyl) propanoic acid (166 mg, 1 mmol), 5e was obtained (166 mg, 40% yield, white powder) ^{1}H NMR ($CDCl_3$): δ 10.79 (br s, OH, 1H), 7.25 (d, J = 8.7 Hz, 2H), 7.04 (d, J = 8.4 Hz, 2H), 2.99 (td, J = 15.6 Hz and J = 7.8 Hz, 2H), 2.70 (td, J = 15.3 Hz and J = 7.2 Hz, 2H), 2.32 (s, 3H).

(E)-3-(3,4-diacetoxyphenyl) acrylic acid (6c). Starting from caffeic acid (2 mmol), 6c was obtained (161 mg, 30% yield, white powder) ^{1}H NMR ($CDCl_3$): δ 7.59 (d, J = 15.9 Hz, 1H), 7.33 (d, J = 8.4 Hz, 1H), 7.64 (d, J = 2.1 Hz, 1H), 7.67 (d, J = 3 Hz, 1H), 6.56 (d, J = 16.2 Hz, 1H), 2.31 (d, J = 2.4 Hz, 6H). DCI-MS (*m/z*): 283.0 (MH^+).

General procedure for the synthesis of compounds 1a, 1b, 1c, 1d, 2a, 2b, 3a, 3b, and 3c. Jaeschkenadiol (419.5 mmol) was dissolved under stirring at room temperature in CH_2Cl_2 (600 mL). The resulting solution was added with corresponding acid (587.3 mmol) and DMAP (125.9 mmol). The solution was left under stirring for 10 min to complete reagents dissolution, and then, *N*,*N*'-dicyclohexylcarbodiimide (DCC, 755.1 mmol) was added. The reaction was complete after 2 h. The solution was concentrated to two volumes (200 mL) and diluted with five volumes of CH_3CN (500 mL); thereafter, the dicyclohexylurea precipitate was filtered off and washed with five more volumes of CH_3CN (250 mL). The combined organic phases were poured into a separatory funnel, extracted with 10% w/v Na_2CO_3 (250 mL) and with a NaCl saturated solution (250 mL), and then dried over Na_2SO_4 (100 g). Na_2SO_4 was filtered off, and the solvent was evaporated under vacuum to give the desired compound.

3-hydroxy-3-isopropyl-6, 8a-dimethyl-1, 2, 3, 3a, 4, 5, 8, 8a-octahydroazulen-4-yl 4-tert-butoxybenzoate (1a). Starting from jaeschkenadiol (100 mg, 0.419 mmol) and 4a acid (130 mg, 0.671 mmol), 1a was obtained (58.6 mg, 35% yield, oil); IR (cm^{-1}): 3477.55, 1692.33, 1603.92, 1272.72, 1253.02, 1154.72. ^{1}H NMR($CDCl_3$) δ 7.93 (d, J = 8.7 Hz, 2H), 7.03 (d, J = 9 Hz, 2H), 5.44 (br s, 1H), 3.91 (td, J = 2.5 Hz and J = 12.5 Hz, 1H), 2.31 (br t, 1H), 2.18 (dd, J = 3 Hz and J = 14.5 Hz, 1H), 2.10 (sept, J = 6.5 Hz, 1H), 1.96 (dd, J = 6 Hz and J = 14.5 Hz, 1H), 1.93 (dd, J = 8 Hz and J = 14 Hz, 1H), 1.80–1.83 (m, 1H), 1.76 (s, 3H), 1.66 (d, J = 10.5 Hz, 1H), 1.55 (td, J = 8 Hz and J = 14 Hz, 1H), 1.42 (dd, J = 7.5 Hz and J = 12.5 Hz, 1 H), 1.16 (ddd, J = 8.5 Hz and J = 12.5 Hz, 1H), 1.10 (s, tBu, 9H), 0.97 (s, 3H), 0.92 (d, J = 7 Hz, 3H), 0.88 (d, J = 7 Hz, 3H); ^{13}C NMR ($CDCl_3$) δ 17.5, 18.6, 20.2, 26.5, 28.9, 29.8, 31.7, 37.3, 41.0, 41.3, 41.4, 44.0, 60.1, 71.1, 86.4, 122.4, 124.5, 125.2, 131.0, δ 133.6, 160.4, 166.5; DCI-MS (*m/z*): 397.2 (MH^+). HRMS (DCI) calcd for $C_{26}H_{37}O_4$: 397.2743, found: 397.2755 (MH^+).

3-hydroxy-3-isopropyl-6, 8a-dimethyl-1, 2, 3, 3a, 4, 5, 8, 8a-octahydroazulen-4-yl 4-(pivaloyloxy) benzoate (1b). Starting from jaeschkenadiol (50 mg, 0.209 mmol) and 4b acid (65 mg, 0.293 mmol), 1b was obtained (90.4 mg, 98% yield, white powder); IR (cm^{-1}): 3478.21,

1747.35, 1755.62, 1705.26, 1684.09, 1604.55, 1279.63, 1108.53. ^{1}H NMR($CDCl_3$) δ 8.04 (d, J = 8.7 Hz, 2H), 7.16 (d, J = 9 Hz, 2H), 5.44 (br s, 1H), 3.91 (td, J = 2.5 Hz and J = 12.5 Hz, 1H), 2.31 (br t, 1H), 2.18 (dd, J = 3 Hz and J = 14.5 Hz, 1H), 2.10 (sept, J = 6.5 Hz, 1H), 1.96 (dd, J = 6 Hz and J = 14.5 Hz, 1H), 1.93 (dd, J = 8 Hz and J = 14 Hz, 1H), 1.80–1.83 (m, 1H), 1.76 (s, 3H), 1.66 (d, J = 10.5 Hz, 1H), 1.55 (td, J = 8 Hz and J = 14 Hz, 1H), 1.42 (dd, J = 7.5 Hz and J = 12.5 Hz, 1H), 1.40 (s, tBu, 9H), 1.16 (ddd, J = 8.5 Hz and J = 12.5 Hz, 1H), 0.97 (s, 3H), 0.92 (d, J = 7 Hz, 3H), 0.88 (d, J = 7 Hz, 3H); ^{13}C NMR ($CDCl_3$) δ 17.5, 18.5, 20.2, 26.5, 27.1, 31.8, 37.3, 39.2, 41.0, 41.3, 41.3, 44.0, 59.9, 71.6, 83.3, 121.7, 121.8, 125.3, 124.0, 127.8, 128.2, 133.6, 155.0, 165.9, 176.6; DCI-MS (*m/z*): 425.2 (M-H_2O). HRMS (DCI) calcd for $C_{27}H_{37}O_3$: 425.2692, found: 425.2700 (M-H_2O).

3-hydroxy-3-isopropyl-6, 8a-dimethyl-1, 2, 3, 3a, 4, 5, 8, 8a-octahydroazulen-4-yl 4-fluorobenzoate (1c). Starting from jaeschkenadiol (50 mg, 0.209 mmol) and 4-fluorobenzoic acid (41 mg, 0.293 mmol), 1c was obtained (48.6 mg, 65% yield, amorphous foam); IR (cm^{-1}): 3513.02, 1700.26, 1604.03, 1469.26, 1271.79, 1238.99. ^{1}H NMR($CDCl_3$) δ 8.04 2d (J = 5.4 Hz and J = 5.4 Hz, 2H), 7.13 2d (J = 8.4 Hz and J = 8.4 Hz, 2H), 5.44 (br s, 1H), 3.91 (td, J = 2.5 Hz and J = 12.5 Hz, 1H), 2.31 (br t, 1H), 2.18 (dd, J = 3 Hz and J = 14.5 Hz, 1H), 2.10 (sept, J = 6.5 Hz, 1H), 1.96 (dd, J = 6 Hz and J = 14.5 Hz, 1H), 1.93 (dd, J = 8 Hz and J = 14 Hz, 1H), 1.80–1.83 (m, 1H), 1.76 (s, 3H), 1.66 (d, J = 10.5 Hz, 1H), 1.55 (td, J = 8 Hz and J = 14 Hz, 1H), 1.42 (dd, J = 7.5 Hz and J = 12.5 Hz, 1H), 1.16 (ddd, J = 8.5 Hz and J = 12.5 Hz, 1H), 0.97 (s, 3H), 0.92 (d, J = 7 Hz, 3H), 0.88 (d, J = 7 Hz, 3H); ^{13}C NMR ($CDCl_3$) δ 17.6, 18.6, 20.2, 26.4, 31.4, 37.0, 40.9, 41.2, 41.4, 44.1, 60.1, 71.3, 87.1, 115.6, 115.9, 125.3, 126.7, 132.1, 132.2, 133.5, 165.6, 165.9; DCI-MS (*m/z*): 343.2 (MH^+-H_2O). HRMS (DCI) calcd for $C_{22}H_{28}FO_2$: 343.2073, found: 343.2086 (MH^+- H_2O).

(E)-(3R, 4S, 8aR)- 3-hydroxy-3-isopropyl-6, 8a-dimethyl-1, 2, 3, 3a, 4, 5, 8, 8a-octahydroazulen-4-yl 3-methoxy-4-(pivaloyloxy) benzoate (1d). Starting from jaeschkenadiol (50 mg, 0.209 mmol) and 4d acid (73.9 mg, 0.293 mmol), 1d was obtained (57 mg, 58% yield, amorphous foam); IR (cm^{-1}): 3514, 1758, 1702, 1604, 1285, 1243, 1200, 1176, 1102. ^{1}H NMR($CDCl_3$) δ 7.61–7.64 (m, 2H), 7.07 (d, J = 8.7 Hz, 1H), δ 5.44 (br s, 1H), 3.91 (td, J = 2.5 Hz and J = 12.5 Hz, 1H), 3.85 (s, OMe, 3H), 2.31 (br t, 1H), 2.18 (dd, J1 = 3 Hz and J = 14.5 Hz, 1H), 2.10 (sept, J = 6.5 Hz, 1H), 1.96 (dd, J = 6 Hz and J = 14.5 Hz, 1H), 1.93 (dd, J = 8 Hz and J = 14 Hz, 1H), 1.80–1.83 (m, 1H), 1.76 (s, 3H), 1.66 (d, J = 10.5 Hz, 1H), 1.55 (td, J = 8 Hz and J = 14 Hz, 1H), 1.42 (dd, J = 7.5 Hz and J = 12.5 Hz, 1H), 1.40 (s, tBu, 9H), 1.16 (ddd, J = 8.5 Hz and J = 12.5 Hz, 1H), 0.97 (s, 3H), 0.92 (d, J = 7 Hz, 3H), 0.88 (d, J = 7 Hz, 3H); ^{13}C NMR ($CDCl_3$) δ 17.6, 18.6, 20.2, 26.4, 27.2, 31.9, 32.4, 37.3, 41.3, 41.3, 41.3, 44.1, 56.0, 60.0, 71.6, 86.3, 113.3, 122.5, 124.0, 125.3, 128.9, 133.5, 144.3, 151.2, 165.9, 176.3; HRMS (DCI) calcd for $C_{28}H_{39}O_6$:471.2747, found: 471.2744.

(E)-(3R, 4S, 8aR)- 3-hydroxy-3-isopropyl-6.8a-dimethyl-1, 2, 3, 3a, 4, 5, 8, 8a-octahydroazulen-4-yl 3-(4-fluorophenyl) acrylate (2a). Starting from jaeschkenadiol (50 mg, 0.209 mmol) and 4-fluorocinnamic acid (48.7 mg, 0.293 mmol), 2a was obtained (44.8 mg, 98% yield, amorphous foam); IR (cm^{-1}): 3513.02, 1700.26, 1604.03, 1469.26, 1271.79, 1238.99. ^{1}H NMR($CDCl_3$) δ 7.65 (d, J = 16.2 Hz, 1H), 7.53 2d (J = 5.4 Hz and J = 5.4 Hz, 2H), 6.32 (d, J = 15.9 Hz, 1H), 7.09 2d (J = 8.7 Hz and J = 8.7 Hz, 2H), 5.44 (br s, 1H), 3.91 (td, J = 2.5 Hz and J = 12.5 Hz, 1H), 2.31 (br t, 1H), 2.18 (dd, J = 3 Hz and J = 14.5 Hz, 1H), 2.10 (sept, J = 6.5 Hz, 1H), 1.96 (dd, J = 6 Hz and J = 14.5 Hz, 1H), 1.93 (dd, J = 8 Hz and J = 14 Hz, 1H), 1.80–1.83 (m, 1H), 1.76 (s, 3H), 1.66 (d, J = 10.5 Hz, 1H), 1.55 (td, J = 8 Hz and J = 14 Hz, 1H), 1.42 (dd, J = 7.5 Hz and J = 12.5 Hz, 1H), 1.16 (ddd, J = 8.5 Hz and J = 12.5 Hz, 1H), 0.97 (s, 3H), 0.92 (d, J = 7 Hz, 3H), 0.88 (d, J = 7 Hz, 3H); ^{13}C NMR ($CDCl_3$) δ 17.6, 18.6, 20.1, 26.5, 31.9, 37.3, 41.0, 41.3, 41.4, 44.0, 60.0, 71.0, 86.3, 116.0, 116.2, 118.0, 118.0, 130.1, 130.5, 130.6, 133.5, 144.1, 164.0, 166.9; DCI-MS (*m/z*): 369.2 (M-OH). HRMS (DCI) calcd for $C_{24}H_{30}FO_2$: 369.2241, found: 369.2230 (M-OH).

3-hydroxy-3-isopropyl-6, 8a-dimethyl-1, 2, 3, 3a, 4, 5, 8, 8a-octahydroazulen-4-yl cinnamate (2b). Starting from jaeschkenadiol (50 mg, 0.209 mmol) and cinnamic acid (43.5 mg, 0.293 mmol), 2b was obtained (53 mg, 98% yield, amorphous foam); IR (cm^{-1}): 3499.45, 1697.94, 1636.01, 1203.57, 1181.47. ^{1}H NMR ($CDCl_3$) δ 7.70 (d, J = 15.9 Hz, 1H), 7.39–7.56 (m, 5 H) 6.40 (d, J = 15.9 Hz, 1H), 5.44 (br s, 1H), 3.91 (td, J = 2.5 Hz and J = 12.5 Hz, 1H), 2.31 (br t, 1H), 2.18 (dd, J = 3 Hz and J = 14.5 Hz, 1H), 2.10 (sept, J = 6.5 Hz, 1H), 1.96 (dd, J = 6 Hz and J = 14.5 Hz, 1H), 1.93 (dd, J = 8 Hz and J = 14 Hz, 1H), 1.80–1.83 (m, 1H), 1.76 (s, 3H), 1.66 (d, J = 10.5 Hz, 1H), 1.55 (td, J = 8 Hz and J = 14 Hz, 1H), 1.42 (dd, J = 7.5 Hz and J = 12.5 Hz, 1H), 1.16 (ddd, J = 8.5 Hz and J = 12.5 Hz, 1H), 0.97 (s, 3H), 0.92 (d, J = 7 Hz, 3H), 0.88 (d, J = 7 Hz, 3H); ^{13}C NMR ($CDCl_3$) δ 17.6, δ 18.6, 20.1, 26.5, 31.8, 37.3, 41.0, 41.3, 41.4, 44.0, 60.1, 70.9, 86.4, 118.2, 125.2, 128.3, 128.9, 130.5, 134.3, 133.6, 145.5, 167.1; DCI-MS (*m/z*): 369.2 (M-H^+). HRMS (DCI) calcd for $C_{24}H_{33}O_3$: 369.2430, found: 369.2435 (M-H^+).

(E)-(3R, 4S, 8aR)- 3-hydroxy-3-isopropyl-6, 8a-dimethyl-1, 2, 3, 3a, 4, 5, 8, 8a-octahydroazulen-4-yl 3-(4-fluorophenyl) propanoate (3a). Starting from jaeschkenadiol (50 mg, 0.209 mmol) and 3-(4-fluorophenyl) propionic acid (49 mg, 0.293 mmol), 3a was obtained (59 mg, 73% yield, amorphous foam); IR (cm^{-1}): 3524,

1717, 1603, 1451, 1156. ^{1}H NMR($CDCl_3$) δ 7.11 2d (J = 5.4 Hz and J = 5.4 Hz, 2H), 6.97 2d (J = 8.7 Hz and J = 8.7 Hz, 2H), 5.44 (br s, 1H), 3.91 (td, J = 2.5 Hz and J = 12.5 Hz, 1H), 2.91 (m, 2H), 2.58 (m, 2H), 2.31 (br t, 1H), 2.18 (dd, J = 3 Hz and J = 14.5 Hz, 1H), 2.10 (sept, J = 6.5 Hz, 1H), 1.96 (dd, J = 6 Hz and J = 14.5 Hz, 1H), 1.93 (dd, J = 8 Hz and J = 14 Hz, 1H), 1.80–1.83 (m, 1H), 1.76 (s, 3H), 1.66 (d, J = 10.5 Hz, 1H), 1.55 (td, J = 8 Hz and J = 14 Hz, 1H), 1.42 (dd, J = 7.5 Hz and J = 12.5 Hz, 1H), 1.16 (ddd, J = 8.5 Hz and J = 12.5 Hz, 1H), 0.97 (s, 3H), 0.92 (d, J = 7 Hz, 3H), 0.88 (d, J = 7 Hz, 3H); ^{13}C NMR ($CDCl_3$) δ 17.6, 18.6, 20.2, 26.4, 30.0, 36.6, 31.4, 37.0, 40.9, 41.2, 41.4, 44.1, 60.1, 71.3, 87.1, 115.2, 115.4, 125.3, 129.7, 129.8, 133.5, 136.0, 161.5, 172.6; DCI-MS (*m/z*): 371.2 (M-OH). HRMS (DCI) calcd for $C_{24}H_{32}FO_2$: 371.2386, found: 371.2374 (M-OH).

(E)-(3R, 4S, 8aR)- 3-hydroxy-3-isopropyl-6, 8a-dimethyl-1, 2, 3, 3a, 4, 5, 8, 8a-octahydroazulen-4-yl-3-phenylpropanoate (3b). Starting from jaeschkenadiol (50 mg, 0.209 mmol) and 3-phenyl propanoic acid (44 mg, 0.293 mmol), 3b was obtained (74.4 mg, 98% yield, amorphous foam); IR (cm^{-1}): 3436, 1728, 1497, 1455, 1385, 1150. ^{1}H NMR($CDCl_3$) δ 7.19–7.32 (m, 5 H), 5.44 (br s, 1H), 3.91 (td, J = 2.5 Hz and J = 12.5 Hz, 1H), 2.95 (t, J = 8.1 Hz, 2H), 2.62 (t, J = 7.8 Hz, 2H), 2.31 (br t, 1H), 2.18 (dd, J = 3 Hz and J = 14.5 Hz, 1H), 2.10 (sept, J = 6.5 Hz, 1H), 1.96 (dd, J = 6 Hz and J = 14.5 Hz, 1H), 1.93 (dd, J = 8 Hz and J = 14 Hz, 1H), 1.80–1.83 (m, 1H), 1.76 (s, 3H), 1.66 (d, J = 10.5 Hz, 1H), 1.55 (td, J = 8 Hz and J = 14 Hz, 1H), 1.42 (dd, J = 7.5 Hz and J = 12.5 Hz, 1H), 1.16 (ddd, J = 8.5 Hz and J = 12.5 Hz, 1H), 0.97 (s, 3H), 0.92 (d, J = 7 Hz, 3H), 0.88 (d, J = 7 Hz, 3H); ^{13}C NMR ($CDCl_3$) δ 17.5, 18.5, 19.9, 26.5, 30.9, 32.0, 36.6, 37.2, 40.9, 41.2, 41.3, 43.9, 59.8, 70.8, 86.2, 126.4, 125.0, 128.3, 128.6, 133.5, 140.4, 172.8; DCI-MS (*m/z*): 369.2 (MH^+). HRMS (DCI) calcd for $C_{24}H_{33}O_3$: 369.2430, found: 369.2440 (MH^+).

(E)-(3R, 4S, 8aR)-3-hydroxy-3-isopropyl-6, 8a-dimethyl-1, 2, 3, 3a, 4, 5, 8, 8a-octahydroazulen-4-yl 3-(4-acetoxyphenyl) propanoate (3c). Starting from jaeschkenadiol (50 mg, 0.209 mmol) and 6c acid (122 mg, 0.586 mmol), 3c was obtained (128 mg, 72%, amorphous foam); IR (cm^{-1}): 3575, 1764, 1722, 1446, 1175; ^{1}H NMR ($CDCl_3$) δ 7.23 (d, J = 8.7 Hz, 2H), 7.02 (d, J = 8.7 Hz, 2H), δ 5.44 (br s, 1H), 3.91 (td, J = 2.5 Hz and J = 12.5 Hz, 1H), 2.96 (m, 2H), 2.61 (m, 2H), 2.31 (br t, 1H), 2.18 (dd, J1 = 3 Hz and J = 14.5 Hz, 1H), 2.30 (s, 3H), 2.10 (sept, J = 6.5 Hz, 1H), 1.96 (dd, J = 6 Hz and J = 14.5 Hz, 1H), 1.93 (dd, J = 8 Hz and J = 14 Hz, 1H), 1.80–1.83 (m, 1H), 1.76 (s, 3H), 1.66 (d, J = 10.5 Hz, 1H), 1.55 (td, J = 8 Hz and J = 14 Hz, 1H), 1.42 (dd, J = 7.5 Hz and J = 12.5 Hz, 1H), 1.16 (ddd, J = 8.5 Hz and J = 12.5 Hz, 1H), 0.97 (s, 3H), 0.92 (d, J = 7 Hz, 3H), 0.88 (d, J = 7 Hz, 3H); ^{13}C NMR ($CDCl_3$) δ 17.4, 18.4, 20.0, 21.1, 26.5, 30.2, 32.2, 36.5, 37.2, 40.9, 41.2, 41.3, 43.9, 59.8, 70.8, 86.2, 121.6, 125.0, 129.3, 133.5, 138.0, 149.1, 169.6, 172.6; HRMS (ESI) calcd for $C_{26}H_{36}O_5Na$: 451.2450, found: 451.2450.

General procedure for the synthesis of compounds ferutinin, 1d', 2c', 2d', 2e', and 3c'. Jaeschkenadiol (419.5 mmol) was dissolved under stirring at room temperature in CH_2Cl_2 (600 mL). The resulting solution was added with corresponding acid (587.3 mmol) and DMAP (125.9 mmol). The solution was left under stirring for 10 min to complete reagents dissolution, and then, N, N'-dicyclohexylcarbodiimide (DCC, 755.1 mmol) was added. The reaction was complete after 2 h. The solution was concentrated to 2 volumes (200 mL) and diluted with 5 volumes of CH_3CN (500 mL); thereafter, the dicyclohexylurea precipitate was filtered off and washed with five more volumes of CH_3CN (250 mL). The combined organic phases were poured into a separatory funnel, extracted with 10% w/v Na_2CO_3 (250 mL) and with a NaCl saturated solution (250 mL), and then dried over Na_2SO_4 (100 g). Na_2SO_4 was filtered off, and the solvent was evaporated under vacuum to give the intermediate compound X.

Compound X was dissolved under stirring at room temperature in 2 L of CH_2Cl_2. The resulting solution was added with ethylenediamine (280 mL). After 3 h, the reaction was complete. The solution was cooled to 0 °C, poured into a separatory funnel, and then washed with 3M H_2SO_4 at 0 °C (750 mL) and a saturated NaCl solution (500 mL). The organic phase was dried over Na_2SO_4 (100 g), filtered, and evaporated to dryness. The residue was purified using flash chromatography, and then, the solvent was evaporated to give the desired compound.

(3R, 4S, 8aR)-3-hydroxy-3-isopropyl-6, 8a-dimethyl-1, 2, 3, 3a, 4, 5, 8, 8a-octahydroazulen-4-yl 4-hydroxybenzoate (ferutinin). Starting from jaeschkenadiol (50 mg, 0.209 mmol) and 4b acid (65 mg, 0.293 mmol), 1 was obtained (90.4 mg, 62% yield, white powder); IR (cm^{-1}): 3385, 1685, 1609, 1312, 1277. ^{1}H NMR ($CDCl_3$) δ 7.94 (d, J = 9 Hz, 2H), 6.92 (d, J = 9 Hz, 2H), 5.44 (br s, 1H), 3.91 (td, J = 2.5 Hz and J = 12.5 Hz, 1H), 2.31 (br t, 1H), 2.18 (dd, J = 3 Hz and J = 14.5 Hz, 1H), 2.10 (sept, J = 6.5 Hz, 1H), 1.96 (dd, J = 6 Hz and J = 14.5 Hz, 1H), 1.93 (dd, J = 8 Hz and J = 14 Hz, 1H), 1.80–1.83 (m, 1H), 1.76 (s, 3H), 1.66 (d, J = 10.5 Hz, 1H), 1.55 (td, J = 8 Hz and J = 14 Hz, 1H), 1.42 (dd, J = 7.5 Hz and J = 12.5 Hz, 1H), 1.16 (ddd, J = 8.5 Hz and J = 12.5 Hz, 1H), 0.97 (s, 3H), 0.92 (d, J = 7 Hz, 3H), 0.88 (d, J = 7 Hz, 3H); ^{13}C NMR ($CDCl_3$) δ 17.6, 18.6, 20.2, 26.4, δ 31.4, 37.0, 40.9, 41.2, 41.4, 44.1, 60.1, 71.3, 87.1, 115.5, 122.0, 125.3, 132.1, 133.5, 161.1,

167.4; DCI-MS (*m/z*): 359.2 (MH^+). HRMS (DCI) calcd for $C_{22}H_{31}O_4$: 359.2222, found: 359.2221 (MH^+).

(3R, 4S, 8aR)-3-hydroxy-3-isopropyl-6, 8a-dimethyl-1, 2, 3, 3a, 4, 5, 8, 8a-octahydroazulen-4-yl 4-hydroxy-3-methoxybenzoate (1d'). Starting from jaeschkenadiol (50 mg, 0.209 mmol) and 4d acid (73.9 mg, 0.293 mmol), 1d' was obtained (25.6 mg, 60% yield, amorphous foam); IR (cm^{-1}): 3408, 1690, 1596, 1429, 1284, 1103. ^1H NMR ($CDCl_3$) δ 7.60 (d, J = 8.5 Hz, 1H), 7.54 (s, 1H), 6.94 (d, J = 8.5 Hz, 1H), 5.44 (br s, 1H), 3.94 (s, OMe, 3H), 3.91 (td, J = 2.5 Hz and J = 12.5 Hz, 1H), 2.31 (br t, 1H), 2.18 (dd, J = 3 Hz and J = 14.5 Hz, 1H), 2.10 (sept, J = 6.5 Hz, 1H), 1.96 (dd, J = 6 Hz and J = 14.5 Hz, 1H), 1.93 (dd, J = 8 Hz and J = 14 Hz, 1H), 1.80–1.83 (m, 1H), 1.76 (s, 3H), 1.66 (d, J = 10.5 Hz, 1H), 1.55 (td, J = 8 Hz and J = 14 Hz, 1H), 1.42 (dd, J = 7.5 Hz and J = 12.5 Hz, 1H), 1.16 (ddd, J = 8.5 Hz and J = 12.5 Hz, 1H), 0.97 (s, 3H), 0.92 (d, J = 7 Hz, 3H), 0.88 (d, J = 7 Hz, 3H); ^{13}C NMR ($CDCl_3$) δ 17.6, 18.6, 20.2, 26.4, 31.4, 37.0, 40.9, 41.2, 41.4, 44.1, 56.0, 60.1, 71.3, 87.1, 114.2, 111.8, 122.5, 124.2, 125.3, 133.5, 146.3, 150.2, 166.4; DCI-MS (*m/z*): 387.2 ($M\text{-}H^+$). HRMS (DCI) calcd for $C_{23}H_{31}O_5$: 387.2171, found: 387.2183 ($M\text{-}H^+$).

(E)-(3R, 4S, 8aR)- 3-hydroxy-3-isopropyl-6, 8a-dimethyl-1, 2, 3, 3a, 4, 5, 8, 8a-octahydroazulen-4-yl 3-(4-hydroxyphenyl) acrylate (2c'). Starting from jaeschkenadiol (50 mg, 0.209 mmol) and 5c acid (73 mg, 0.293 mmol), 2c' was obtained (30 mg, 37% yield, amorphous foam); IR (cm^{-1}): 3408, 1690, 1596, 1429, 1284. ^1H NMR($CDCl_3$) δ 7.67 (d, J = 16 Hz, 1H), 7.47 (d, J = 8.5 Hz, 2H), 6.88 (d, J = 8.5 Hz, 2H), 6.28 (d, J = 16 Hz, 1H), 5.44 (br s, 1H), 3.91 (td, J = 2.5 Hz and J = 12.5 Hz, 1H), 2.31 (br t, 1H), 2.18 (dd, J = 3 Hz and J = 14.5 Hz, 1H), 2.10 (sept, J = 6.5 Hz, 1H), 1.96 (dd, J = 6 Hz and J = 14.5 Hz, 1H), 1.93 (dd, J = 8 Hz and J = 14 Hz, 1H), 1.80–1.83 (m, 1H), 1.76 (s, 3H), 1.66 (d, J = 10.5 Hz, 1H), 1.55 (td, J = 8 Hz and J = 14 Hz, 1H), 1.42 (dd, J = 7.5 Hz and J = 12.5 Hz, 1H), 1.16 (ddd, J = 8.5 Hz and J = 12.5 Hz, 1H), 0.97 (s, 3H), 0.92 (d, J = 7 Hz, 3H), 0.88 (d, J = 7 Hz, 3H); ^{13}C NMR ($CDCl_3$) δ 17.6, 18.6, 20.1, 26.5, 31.7, 37.3, 41.0, 41.2, 41.4, 44.0, 60.1, 70.8, 86.6, 115.4, 116.0, 125.2, 126.9, 130.2, 133.6, 145.4, 158.1, 167.7; DCI-MS (*m/z*): 385.2 (MH^+). HRMS (DCI) calcd for $C_{24}H_{33}O_4$: 385.2379, found: 385.2386 (MH^+).

(E)-(3R, 4S, 8aR)- 3-hydroxy-3-isopropyl-6, 8a-dimethyl-1, 2, 3, 3a, 4, 5, 8, 8a-octahydroazulen-4-yl 3-(4-hydroxy-3-methoxyphenyl) acrylate (2d'). Starting from jaeschkenadiol (50 mg, 0.209 mmol) and 5d acid (81.5 mg, 0.293 mmol), 2d' was obtained (38.2 mg, 71% yield, amorphous foam); IR (cm^{-1}): 3415, 1689, 1629, 1268, 1172. ^1H NMR($CDCl_3$) δ 7.65 (d, J = 16 Hz, 1H), 7.12 (dd, J = 1.5 Hz and J = 8.5 Hz, 1H), 7.06 (d, J = 2 Hz, 1H), 6.96 (d, J = 8.5 Hz, 1H), 6.27 (d, J = 16 Hz, 1H), 5.44 (br s, 1H), 3.91 (td, J = 2.5 Hz and J = 12.5 Hz, 1H), 2.31 (br t, 1H), 2.18 (dd, J = 3 Hz and J = 14.5 Hz, 1H), 2.10 (sept, J = 6.5 Hz, 1H), 1.96 (dd, J = 6 Hz and J = 14.5 Hz, 1H), 1.93 (dd, J = 8 Hz and J = 14 Hz, 1H), 1.80–1.83 (m, 1H), 1.76 (s, 3H), 1.66 (d, J = 10.5 Hz, 1H), 1.55 (td, J = 8 Hz and J = 14 Hz, 1H), 1.42 (dd, J = 7.5 Hz and J = 12.5 Hz, 1H), 1.16 (ddd, J = 8.5 Hz and J = 12.5 Hz, 1H), 0.97 (s, 3H), 0.92 (d, J = 7 Hz, 3H), 0.88 (d, J = 7 Hz, 3H); ^{13}C NMR ($CDCl_3$) δ 17.6, 18.6, 20.1, 26.5, 31.7, 37.3, 41.0, 41.3, 41.5, 44.0, 56.0, 60.1, 70.7, 86.3, 109,5, 114.7, 115.5, 125.2, 126.8, 123.2, 133.6, 145.6, 146.8, 148.1, 167.5; DCI-MS (*m/z*): 415.2 (MH^+). HRMS (DCI) calcd for $C_{25}H_{35}O_5$: 415.2484, found: 415.2476 (MH^+).

(E)-(3R, 4S, 8aR)- 3-hydroxy-3-isopropyl-6, 8a-dimethyl-1, 2, 3, 3a, 4, 5, 8, 8a-octahydroazulen-4-yl)-3-(3, 4 dihydroxyphenyl) acrylate (2e'). Starting from jaeschkenadiol (50 mg, 0.209 mmol) and 5e acid (73.9 mg, 0.293 mmol), 2e' was obtained (22.5 mg, 27% yield, green oil); IR (cm^{-1}): 3373, 1682, 1674, 1633, 1601, 1178. ^1H NMR($CDCl_3$): δ 7.74 (d, 15.9 Hz, 1H), 7.21 (d, 1.8 Hz, 1H), 7.06 (dd, J = 1.8 Hz and J = 8.4 Hz, 1H), 6.92 (d, 8.1 Hz, 1H), 6.57 (d, 15.9 Hz, 1H), 5.44 (br s, 1H), 3.91 (td, J = 2.5 Hz and J = 12.5 Hz, 1H), 2.31 (br t, 1H), 2.18 (dd, J = 3 Hz and J = 14.5 Hz, 1H), 2.10 (sept, J = 6.5 Hz, 1H), 1.96 (dd, J = 6 Hz and J = 14.5 Hz, 1H), 1.93 (dd, J = 8 Hz and J = 14 Hz, 1H), 1.80–1.83 (m, 1H), 1.76 (s, 3H), 1.66 (d, J = 10.5 Hz, 1H), 1.55 (td, J = 8 Hz and J = 14 Hz, 1H), 1.42 (dd, J = 7.5 Hz and J = 12.5 Hz, 1H), 1.16 (ddd, J = 8.5 Hz and J = 12.5 Hz, 1H), 0.97 (s, 3H), 0.92 (d, J = 7 Hz, 3H), 0.88 (d, J = 7 Hz, 3H); ^{13}C NMR ($CDCl_3$) δ 17.7, 18.6, 20.2, 26.3, 31.2, 36.8, 40.9, 41.1, 41.7, 44.3, 60.5, 71.4, 87.8, 114.2, 114.6, 115.0, 122.2, 125.5, 126.8, 133.4, 144.4, 147.0, 147.7, 169.8; DCI-MS (*m/z*): 401.2 (MH^+). HRMS (DCI) calcd for $C_{24}H_{33}O_5$: 401.2328, found: 401.2342 (MH^+).

(E)-(3R, 4S, 8aR)- 3-hydroxy-3-isopropyl-6, 8a-dimethyl-1, 2, 3, 3a, 4, 5, 8, 8a-octahydroazulen-4-yl 3-(4-hydroxyphenyl) propanoate (3c'). Starting from jaeschkenadiol (100 mg, 0.420 mmol) and 6c acid (122 mg, 0.586 mmol), 3c' was obtained (108 mg, 67% yield, amorphous foam); IR υmax cm^{-1}: 3388, 1712, 1615, 1450, 1150. ^1H NMR($CDCl_3$) δ 7.10 (d, J = 8.4 Hz, 2H), 6.79 (d, J = 8.4 Hz, 2H), 5.44 (br s, 1H), 3.91 (td, J = 2.5 Hz and J = 12.5 Hz, 1H), 2.92 (m, 2H), 2.60 (m, 2H), 2.31 (br t, 1H), 2.18 (dd, J = 3 Hz and J = 14.5 Hz, 1H), 2.10 (sept, J = 6.5 Hz, 1H), 1.96 (dd, J = 6 Hz and J = 14.5 Hz, 1H), 1.93 (dd, J = 8 Hz and J = 14 Hz, 1H), 1.80–1.83 (m, 1H), 1.76 (s, 3H), 1.66 (d, J = 10.5 Hz, 1H), 1.55 (td, J = 8 Hz and J = 14 Hz, 1H), 1.42 (dd, J = 7.5 Hz and J = 12.5 Hz, 1H), 1.16 (ddd, J = 8.5 Hz and J = 12.5 Hz, 1H), 0.97 (s, 3H), 0.92 (d, J = 7 Hz, 3H), 0.88 (d, J = 7 Hz, 3H); ^{13}C NMR ($CDCl_3$) δ 17.5, 18.5, 20.0, 26.5, 30.0, 31.8, 37.0, 37.2, 40.9, 41.3, 41.3, 43.9, 59.8, 70.9, 86.5, 115.5, 125.0, 129.4, 132.3, 133.5,

154.3, 173.0; DCI-MS (*m/z*): 386.2. HRMS (DCI) calcd for $C_{24}H_{34}O_4$: 386.2457, found: 386.2453.

Biology

Cell culture

MCF-7, estrogen receptor-positive, and MDA-MB-231, estrogen receptor-negative, human breast cancer cell lines, purchased originally from ATCC, were routinely maintained in RPMI 1640 medium (Lonza, Basel, Switzerland) supplemented with 10% v/v fetal bovine serum (Sigma, St Louis, MO, USA), 1% v/v antibiotics agents (penicillin streptomycin) (Sigma). MCF-10A cells were originally purchased from ATCC and grown in Ham's F12: DMEM (50:50), 2.5 mM L-glutamine, 20 ng/mL epidermal growth factor (EGF) (Sigma), 0.1 μg/mL cholera toxin (CT) (Sigma), 10 μg/mL insulin (Sigma), 500 ng/mL hydrocortisone (Sigma), and 5% horse serum. HAEC cells were purchased from Lonza, USA. They were cultured in medium M199, enriched with 20% fetal calf serum (FCS), bovine hypothalamic growth factor (ECGF), and heparin. Cells were split once a week and used for experiments between passages 1 to 8. The four cell lines were grown to confluence at 37 °C in a humidified atmosphere containing 5% CO_2 in air and were passaged weekly using 1% trypsin (Gibco, USA) to maintain the optimum conditions for exponential growth.

Cell proliferation assay

The antiproliferative activities of target compound were determined using standard MTT cell proliferation assay (Promega, USA). This is a colorimetric assay that depends on the cellular reduction of MTT to a blue formazan product by the mitochondrial dehydrogenase of viable cells. The optical density of the blue color is a measure of cell viability.

MCF-7 and MDA-MB-231 cells were cultured in 96-well plates with a density of 3000 cells/well. After 24 h, exponentially growing cells were exposed to the compounds in triplicate at final concentrations ranging from 1 to 50 μM. Stock solutions of each compound were freshly prepared in DMSO, diluted with cell culture medium and filter sterilized with a 0.22 μm syringe filter. The highest concentration of DMSO following dilution was 0.75% of the total volume, an amount that was not toxic to the cells. Control wells received medium with DMSO, without the tested compound. After 24, 48, and 72 h of incubation, 5 mg/mL of MTT reagent was added and cultured for 4 h, and then, solubilization solution was added (100 mL/well). The optical density is measured, after 24 h of incubation, at 570 nm by the Multiskan Ex spectrum. Results are presented as the average of three wells. The percent of cells surviving was determined by comparing the average absorbance with the standard deviation (SD) of three wells/concentration of the treated cells with the average absorbance SD of three wells/concentration of the non-treated cells. Results are presented as percent of control. The final results were obtained in one independent experiment run in triplicate.

Western blotting

Cellular protein extracts were prepared and quantified using DC Bio-Rad protein assay kit (Bio-Rad, Hercules, CA, USA) as per manufacturer's recommendations employing bovine serum albumin (BSA) as a standard. Whole cell lysates (100 μg) were separated by SDS–PAGE (12%), transferred to PVDF membranes (Bio-Rad), and probed with anti-phosphor-Ser 118 ERα antibodies (GeneTex, San Antonio, TX, USA), followed by horseradish peroxidase-conjugated anti-rabbit IgG-HRP (Santa-Cruz, CA, USA). β-Actin (Sigma) was used to assess protein loading. Immune complexes were detected using the ECL chemoluminescent system bands and normalized according to the internal control. Bands were quantified using ImageJ software (Image J Software, Bethesda, MD, USA).

Immunofluorescence staining

Cultured cells on glass coverslips were washed with PBS and fixed in ice-cold methanol overnight. Cells were then washed with PBS and blocked for 1 h at room temperature with 5% normal goat serum (NGS) (Sigma). After incubation overnight at 4 °C with primary antibody against phosphor-Ser 118 ERα (GeneTex), slides were washed three times in PBS. The antibodies were diluted in 1% NGS in PBS, and samples were placed on parafilm in a humidified chamber. The rabbit monoclonal antibody p-ERα (1 mg/mL) was used at 1/1000 dilution. Cells were next incubated with the secondary antibody Alexa Fluor 488 of goat anti-rabbit IgG antibody (1:500, Invitrogen, Carlsbad, CA, USA). Cellular DNA was stained by addition of Hoechst 33258 (Sigma) dye at 0.5 mg/mL after the incubation with the second antibody. Cells incubated without first antibody were included as controls. After washing, the coverslips were mounted on slides with an antifade reagent. Slides were examined using a laser scanning confocal microscopy, LSM710 (Carl Zeiss, Oberkochen, Germany).

Molecular modeling methods

The protein structures used in this paper were taken from the Protein Data Bank (PDB: RSCB Protein Data Bank (http://www.rscb.org/pdb/). Accelrys Discovery Studio Visualizer (DSV, Accelrys Software Inc., DISCOVERY STUDIO MODELING ENVIRONMENT, Release 4.0, San Diego: Accelrys Software Inc., 2013) or SciTE text editor (http://www.scintilla.org/SciTE.html) were used to split the structures in polypeptide chains.

The chains (not only chain A) were structurally aligned with structure 1XPC (chain A) set as reference (defining a reference space) using UCSF Chimera (18)/Matchmaker (19) program. The protein structures in the reference space

were prepared (structure checks, rotamers) using DSV and UCSF Chimera 1.8.1 (DockPrep without minimization, rotamers).

The co-crystallized ligand structures were extracted from protein structures using SciTE and DSV. The compound structures were sketched using CHEMAXON MARVIN 5.5, ChemAxon (http://www.chemaxon.com). The ligands were prepared (hybridization, hydrogenation, some geometry optimizations) and aligned (center of mass) with co-crystallized ligands in the previously defined reference space using DSV, and all ligands and compounds were merged in SDF libraries for import in docking software. The produced SDF libraries were also checked using CHEMAXON MARVIN 5.5 and eventually corrected using previous cited software. Molecular studies (docking, scoring) were carried out with MOLEGRO VIRTUAL DOCKER 6 (MVD) software (http://www.clcbio.com). After structural alignment, the six structures of ERα and five structures of ERβ (defined as canonical in the study) were used for molecular docking (Tables S1 and S2). In each structure, an equivalent search space (volume of 17 Å radius) centered in the binding domain was chosen for docking. Any water molecule (entropy penalty or presence of HOH atoms) was taken into account in this study.

Ligands and binding pocket were set flexible during the calculation. According to structural study, 33 equivalent residues were defined for flexible docking: Ala 350, Arg 394, Glu 323, Glu 353, Gly 390, Gly 521, His 524, Ile 326, Ile 386, Ile 424, Leu 327, Leu 346, Leu 349, Leu 354, Leu 384, Leu 387, Leu 391, Leu 428, Leu 525, Leu 540, Lys 449, Met 343, Met 357, Met 388, Met 421, Phe 404, Phe 425, Phe 445, Pro 324, Thr 347, Trp 360, Trp 383, Trp 393 (typical list for 1G50 structure). A tolerance of 0.99, a flexibility of 0.90, and softened potentials were used, if enabled by docking algorithm. Values of 2000 steps (lateral chains of residues) and 2000 steps (backbone) were used for final minimization (postdocking).

A docking template (seven steric atoms, 1 oxygen donor, 1 oxygen acceptor, six ring carbons as pharmacophore profile) was defined using the phenol group of the estradiol (EST) ligand in ERα and in ERβ. The grid resolution for template was set to 0.4 Å, and other parameters were set as default values. The docking template was used during docking process; the method gave also a similarity score in addition to docking score, but this measure was not useful in this case, another definition of similarity (called 'conformity') was defined and used.

MolDock (20) was used as scoring function with a grid resolution of 0.20 Å. MolDock Optimizer (CPU) or a docking/scoring algorithm GPU/CUDA based (using Nvidia Tesla processors) were used with default values (except a population size of 200 and 5000 steps of calculation by run (MolDock optimizer, CPU). A CUDA score was also produced by the docking process (GPU), but this measure was not used in further analysis.

Each compound was docked iteratively using 10 independent runs by protein structure (11 total structures for ERα and ERβ) and CPU/GPU methods (220 total runs per compound). In the case of ferutinin and co-crystallized ligands, 10 independent docking runs were generally enough to give a limit (asymptotic) value of MolDock score. Finally, a tabu clustering (default values) was used to rank the poses, and final MolDock and Rerank scores were calculated after a postdocking minimization.

The sets of 10 poses were submitted to visual inspection and pose selection. In this case, calculations using GPU methods were more reliable and were used for this study. A filter was used to define the so-called best poses of each set. For scores, the following rules were defined: (i) best (lowest negative values) MolDock and Rerank scores correspond to the same pose; (ii) if not, the best score with the priority Rerank > MolDock was retained. For visual inspection, the following rules were defined: (iii) the presence of one or more H-bonds with Glu305 or Arg346 and an edge to face π–π interaction with Phe404; (iv) a degree of superimposition between the phenol substituted group of the pose (if it exists) and the same chemical group in the co-crystallized structures, typically the phenol ring of œstradiol. These rules were applied with ascending priority (scores > visual inspection) to select the best pose from each set of 10 poses.

The information given by (iii–iv) rules was used to tag all the poses (best or not). The aim was to approach a 'conformity' criterion (analysis of structurally aligned and liganded ER structures show that this kind of interaction and group placement is generally reproduced in co-crystallized complexes) in order to define postdocking descriptors. If the phenol group of the ferutinin derivative is globally aligned in the same way that the phenol group of estradiol (in this case, the conformation of the compound is able to make hydrogen bonds with ARG394 and GLU353 residues), the docking pose was tagged as 'conform'. We defined two indicators for the so-called conformity: *CBP* and *CPC*. The *CBP* was true (+) when the pose corresponding to the best docking score was conform. The *CPC* was defined as the number (0. 10) of conform poses in a set of ten independent docking runs. A *Hit* descriptor was defined at *High* when the (MolDock score <= −100) and (Rerank score <= −50) and (CPC >8) and (*CBP* is positive). To add a range in this switch, the *Hit* descriptor was retained but lowered at *Low* when the previous conditions satisfied except for Rerank score <= 20 or CPC >=5.

Then, all docking data were gathered and used to produce the results of Table 2.

Results and Discussion

Chemistry

The preparation of ferutinin analogues was achieved by hemisynthesis from jaeschkenadiol according to the synthesis of ferutinin previously reported by Bombardelli *et al.* (Scheme 1) (21). *Ferula hermonis* roots were collected from Mount Hermon (Lebanon). Daucane esters were directly obtained from the crude extract of the plant roots and were hydrolyzed into the parent alcohol, jaeschkenadiol.

Jaeschkenadiol was reacted with different carboxylic acids including substituted benzoic, cinnamic, and phenylpropanoic acids to yield 1–3 analogues series, respectively. When carboxylic acids possess a hydroxy substituent on the aromatic ring, it had to be protected as a *tert*-butoxy (**4a**), a pivaloyloxy (**4b**, **4d, 5c,** and **5d**), or an acetoxy group (**5e**, **6c**) to avoid cross-reactivity. Compounds **4a**, **4b,** and **5e** were synthesized according to procedures previously published (22–24). The pivaloyl derivatives **4d**, **5c,** and **5d** were obtained by the action of pivaloyl chloride and DMAP in pyridine, whereas reaction

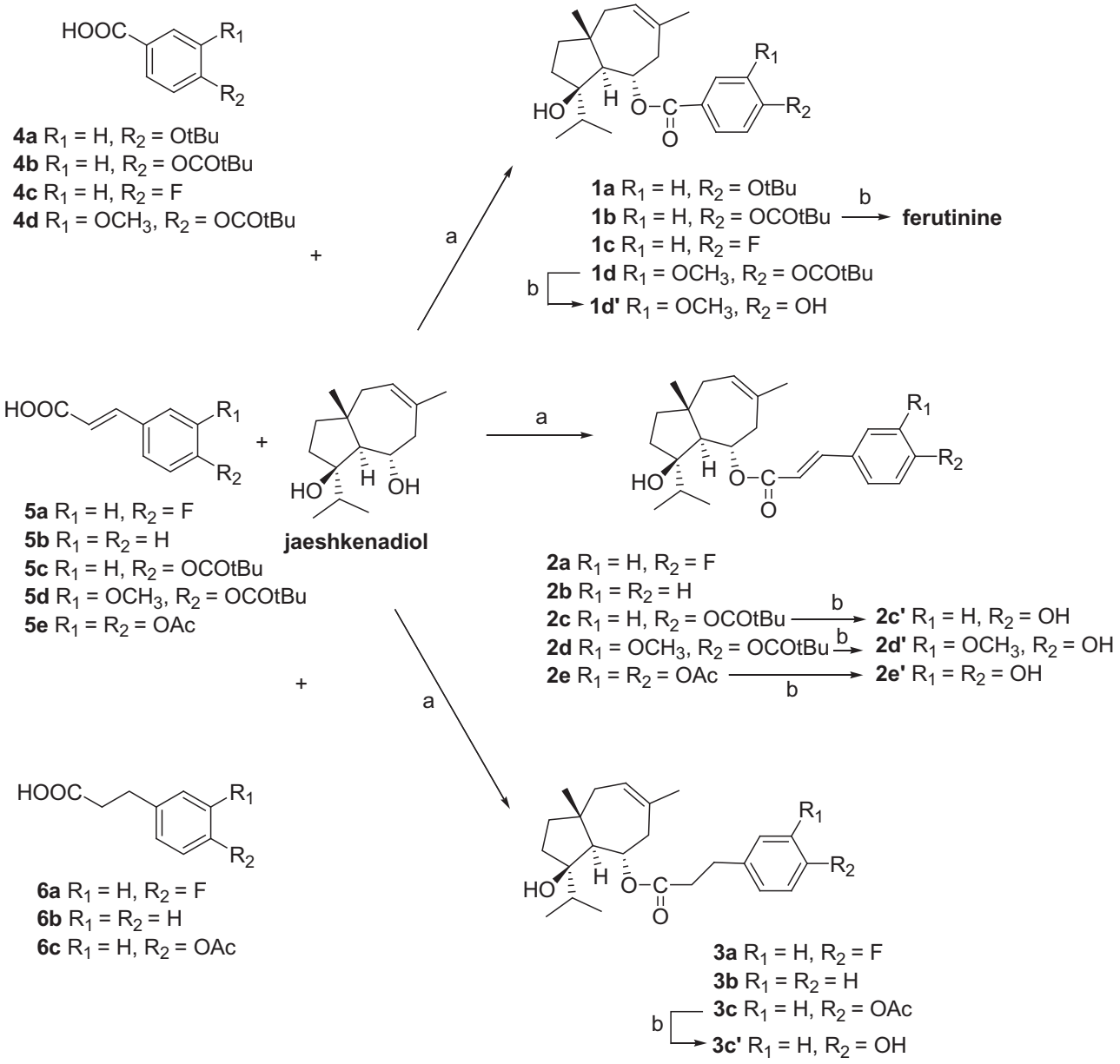

Scheme 1: Synthesis of ferutinin analogues.

of acetic anhydride in pyridine provided the acetoxy-one **6c**. The esterification reactions were carried out at room temperature, in CH_2Cl_2, in the presence of DMAP and DCC which was added to activate corresponding acids. Reactions yields giving **1a-d**, **2a-e,** and **3a-c** derivatives ranged from 35 to 98%. However, no attempt was carried out to optimize the overall yields. The clivage of the protective groups to provide the desired compounds **ferutinin, 1d'**, **2c'-e',** and **3c'** was affected by ethylenediamine's action in CH_2Cl_2. It is noteworthy that the production of ferutinin, initially present at 52% in the crude extract of the plant, was improved up to 62% from jaeschkenadiol obtained from daucane esters hydrolysis.

Antiproliferative activity

The antiproliferative activity of ferutinin and its analogues was assessed by means of the 3-(4,5-dimethylthiazol-2-yl)-2,5-diphenyl tetrazolium bromide (MTT) test, against both estrogen-dependent and estrogen-independent breast cancer cell lines (MCF-7 and MDA-MB-231, respectively). Tamoxifen was used as positive control whereas jaeschkenadiol, isolated from the crude extract of the plant, was used as negative control. The results are given in Table 1. The data clearly show that ferutinin inhibits the proliferation of both cell lines to the same extent.

Even if ferutinin has higher affinity toward ERs than the chemotherapeutic agent currently in use tamoxifen (12), it retains only an agonist activity against ERα, which may explain the difference found in the antiproliferative activity of these two compounds in MCF-7 cells. Tamoxifen, known for its antagonist potential in the breast, remains more potent on the inhibition of the proliferation of MCF-7 cell line (IC_{50} = 10 μM) when comparing to ferutinin (IC_{50} = 38 μM).

Table 1: Antiproliferative activity of ferutinin and hemisynthesized analogues

	IC_{50} (μM)			
Compound	MCF-7	MDA-MB-231	MCF-10A	HAEC
Tamoxifen	10	Nd	Nd	Nd
Jaeschkenadiol	>50	>50	Nd	Nd
Ferutinin	38	28	50	30
1a	>50	>50	Nd	Nd
1b	>50	>50	Nd	Nd
1c	45	>50	Nd	Nd
1d'	25	47	>50	Nd
2a	>50	>50	Nd	Nd
2b	41	>50	>50	Nd
2c'	22	9	48	10
2d'	32	23	>50	Nd
2e'	38	24	Nd	Nd
3a	>50	>50	>50	Nd
3b	>50	>50	Nd	Nd
3c'	**1**	>50	>50	>50

Nd, not determined. IC_{50} values were derived from single dose–response curves generated from triplicate data points. Tamoxifen is taken as a control for estrogen-responsive cell line. MCF-7 is an estrogen-dependent breast cancer cell line; MDA-MB-231 is an estrogen-independent breast cancer cell line. MCF-10A is a mammary epithelial normal cell line. HAEC are primary human aortic endothelial cells. MTT assay was carried out after 72 h of treatment.

In general manner, among the analogues, compounds having a hydroxy moiety on the aromatic ring, **1d'**, **2c'-e'**, exhibited antiproliferative activity on both MCF-7 and MDA-MB-231 cell lines. The data relative to the estrogenic MCF-7 cell line confirmed the crucial role of the hydroxy function capable to form a hydrogen bond in the binding site of estrogen receptors as previously pointed out by Appendino *et al.* (23). Compound **3c'** which has shown the most significant result (one log of magnitude when compared to tamoxifen) was the sole compound among those bearing a hydroxy substituent which revealed an effect on MCF-7 cells but not on the other cell line. The introduction of two carbons with a saturated bond between the carbonyl and the phenol moiety has enhanced the activity of the molecule which has been previously described to have a negligible estrogenic activity compared to ferutinin (EC_{50} <0.0001% and 0.5%, respectively) (13).

Interestingly, the switch into an unsaturated bond in **2c'** versus **3c'** decreased the antiproliferative activity but enhanced it when comparing to ferutinin.

The replacement of the hydroxy group by a more electronegative halogen substituent such as fluorine (compounds **1c**, **2a,** and **3a**) decreased the antiproliferative activity of ferutinin. Moreover, the introduction of an electron-contributing group such as a methoxy group in *meta* position toward the hydroxy function caused a slight increase in the potency as observed for **1d'** and **2d'**.

Concerning the data relative to the estrogen-independent MDA-MB-231 cell line, two compounds **2d'** and **2e'** exert antiproliferative activity of the same order of magnitude than ferutinin (IC_{50} = 23 and 24 μM, respectively), whereas **2c'** shows an improved effect (IC_{50} = 9 μM). Further studies on the signaling pathways induced by this compound could be useful for a better understanding of the molecular mechanism involved in its antiproliferative activity.

In an attempt to obtain more insights into the cytotoxic potential of compounds under study against normal human cells, ferutinin and its most active analogues were assayed *in vitro* against non-tumorigenic breast MCF-10A and normal human endothelial aortic HAEC cells. Results showed that ferutinin is more selective against MCF-7 cell line when compared to the immortalized normal MCF-10A cell line (IC_{50} = 38 versus 50 μM). On the other hand, it induces toxicity on normal HAEC cells. Compound **2c'** had also an antiproliferative effect on HAEC cells but not on MCF-10A cells (IC_{50} = 10 and 48 μM, respectively).

Finally, compound **3c'** selectively induced cell death in MCF-7 cancer cell line, but not in the other three cell lines.

Molecular docking

The molecular target of **3c'** and ferutinin (FRT) on MCF-7 cells was investigated using molecular docking studies on ERα and ERβ. According to previous work on nuclear receptors (25–27), a 4D docking (28) strategy was applied to approach conformational changes inside the binding site.

Using structural alignments of protein-ligand complexes, known in the PDB (Protein Data Bank) database (47 ERα and 33 ERβ in this study), an analysis was performed based (i) on the chemical diversity and activity (agonist–antagonist) of co-crystallized ligands and (ii) correlated variations of binding site's topology. A reduced set of 11 proteins representative (canonical) structures were then generated (6 ERα and 5 ERβ) and used as molecular docking frames.

The 80 PDB protein–ligand complexes issued from initial and canonical ensembles share common structural characteristics. Ligand recognition was achieved through a combination of specific hydrogen bonds and the complementarity of the binding cavity to the non-polar character of each molecule. In both agonist (structures 2P15 (B), 1G50 (A) for ERα) or antagonist (structures 1R5K (A), 1XPC, 2IOG, 3ERT for ERα) ligands, a phenol group was found to have the same orientation and alignment. Inside the binding cavity, this group was oriented toward a gate pointing to another cavity, where a water molecule nestled, and sandwiched between the side chains of structurally conserved ARG and GLU facing residues. Consequently, the phenolic hydroxyl was able to make direct hydrogen bonds with the carboxylate of GLU 353, the guanidinium group of ARG 394, and the water molecule. This group was later on used as a pharmacophore and filter in docking studies. On the other hand, a PHE404 residue was conserved which could interact with aromatic zones of potent ligands. The co-crystallized ligands have also a part of structure that is aligned on the same plane than 'estradiol like' molecules. The binding cavity around estradiol zone and particularly the gate seems to be poorly affected by topologic changes related to the displacement of H12 helix from agonist state (the binding cavity is closed) to antagonist state (opened binding cavity).

Despite these conserved elements among the set of protein–ligand complexes (and whatever local backbone/residue flexibility is used or not by docking algorithms), the 4D docking data analysis remains complex due to the multiplicity of PDB entries used. We have used Molegro Virtual Docker (MVD) with retention of MolDock (20) and Rerank score issued from MVD calculations. The validation of docking algorithms depends upon heterogeneous conformational ensembles that differ from protein–ligand sets. Therefore, docking methods should be used with combination of structural elements (pharmacophores, filters, etc.) related to the problem itself, rather than searching only the best scores. Taking account of that, postdocking descriptors (*CBP*, *CPC,* and *Hit* described in experimental section) were introduced into the calculation system to filter docking results. These descriptors share the ability (i) to produce (*CBP*) a pose (for example phenol group) similar to that obtained with the co-crystallized ligands combined with best scores and (ii) to reproduce (*CPC*) this result for a given number (10) of independent runs. The *Hit* switch summarizes results from scores and descriptors which are used as a low-cut filter, to select significant poses. All docking data for compound **3c'** are depicted in Table 2 (docking scores, postdocking descriptors) and in Figure 2 (docking poses).

In the antagonist position of the ERα (2IOG, 1R5K) and the ERβ (1X7R), poses selected with a value (*High* or *Low*) of *Hit* descriptor shared similar structural elements (ester group, daucane core). In these cases, they were able to fit the C-cavity of the binding site. The

Table 2: Docking results for compound **3c'** in ERα and ERβ structures

Receptor	Canonical	Ligand class	MolDock score	Rerank score	CBP	CPC	Hit
ERα	2IOG	Antagonist	−112.197	−29.0271	+	9	Low
	3ERT	Antagonist	−50.2323	342.431	–	0	–
	1R5K (A)	Antagonist	−120.673	−45.885	+	5	Low
	1XPC	Antagonist	−85.5529	149.04	+	1	–
	1G50 (A)	Agonist	−78.6739	181.361	+	6	–
	2P15 (B)	Agonist	−130.82	−86.0078	–	8	–
ERβ	1QKN	Antagonist	−64.0379	323.455	+	3	–
	1X7R	Agonist/antagonist	−150.37	−103.526	+	10	High
	2YJA	Agonist	−96.0588	108.85	+	8	–
	2IOJ (C)	Agonist	−130.178	−63.9421	+	8	High
	1U3S (A)	Agonist	−123.364	30.8986	+	6	–

Docking scores (arbitrary units) obtained using Molegro Virtual Docker and postdocking descriptors are described in experimental section. Ligand classes are based on the activity (mainly agonist or antagonist) of the co-crystallized ligand found in corresponding PDB structure.

corresponding poses for 2IOG and 1X7R are shown in Figure 2A,B. Compound **3c'** displayed also a *Hit* value in agonist position in the 2IOJ (chain C) structure. The corresponding pose in Figure 2C showed that the binding modes were different from the previous case, particularly due to the fact that the compound fulfilled the C-cavity/β-face without any implication of the ester group and daucane core.

These preliminary results showed that compound **3c'** could eventually interact with both ERα and ERβ. This binding procedure is in favor of an antagonist orientation in both ER subtypes.

To date, no available co-crystallized complexes of ferutinin and ERs are available. Therefore, molecular docking could serve as a first approach for structural understanding of ferutinins' reported functions.

Ferutinin was docked inside the binding domain of each receptor using the same protocol described previously. Results are shown in Table 3 and Figure 3 for ERα and

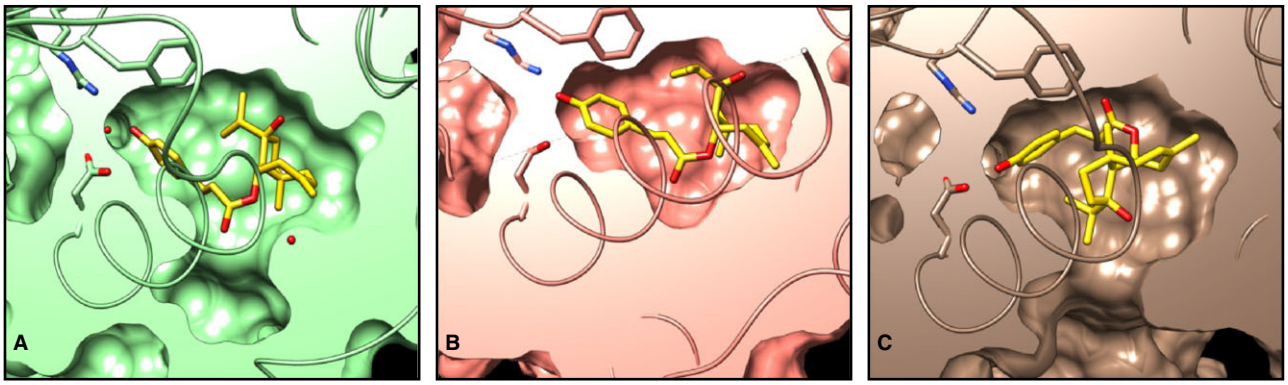

Figure 2: Docking poses of compound **3c'** in ERα/ERβ binding cavities. Docking poses of **3c'** from Table 1 in (A) 2IOG (Chain A, ERα, green); (B) 1X7R (Chain A, ERβ, salmon); and (C) 2IOJ (Chain C, ERβ, brown). The clipping planes of aligned structures are the same, and set using lateral chains of GLU 353 and ARG394 (A-Cavity), PHE 404 is also shown (left-up). The cavity around the upper part of the cavity (occupied by estradiol compound in multiple PDB structures) is labeled α-face, and the subcavity involved in the gate surrounded by ARG, GLU residues is labeled A-cavity. The subcavity at the bottom of closed site (1X7R) is labeled C-cavity; in the case of an opened binding site (2IOJ), the β-face is defined by the bottom part of image.

Table 3: Docking scores of ferutinin in ERα sites

Receptor	Canonical	Ligand class	MolDock score	Rerank score	CPC	CBP	Hit
ERα	2IOG	Antagonist	−92.33	−2.02	10	+	–
	3ERT	Antagonist	359.23	2581.35	0	–	–
	1R5K (A)	Antagonist	−96.97	17.85	7	+	–
	1XPC	Antagonist	−92.35	−8.79	2	–	–
	1G50 (A)	Agonist	−118.20	−57.28	9	+	High
	2P15 (B)	Agonist	−114.07	−81.05	9	+	High

Docking scores (arbitrary units) obtained using Molegro Virtual Docker, and postdocking descriptors are described in experimental section. Ligand classes are based on the activity (mainly agonist or antagonist) of the co-crystallized ligand found in corresponding PDB structure.

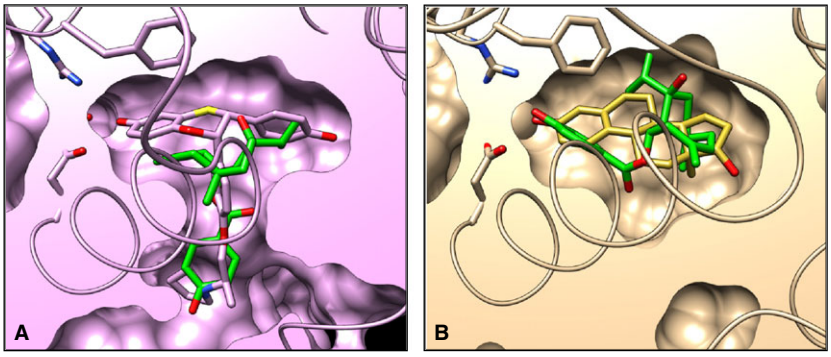

Figure 3: Docking poses of Ferutinin in ERα binding cavities. Ferutinin (FRT, green) docking poses from Table 3 are shown in 1G50 (A, chain A, ERα, brown, closed cavity) and 1XPC (B, chain A, ERα, purple, opened cavity) structures, including the corresponding co-crystallized ligands EST (gold, agonist) and AIT (purple, antagonist). The clipping planes of aligned structures are the same, and set using lateral chains of GLU 353 and ARG394 (left), PHE 404 is also shown (left-up).

Table 4 and Figure 4 for ERβ. Ferutinins' docking results are difficult to interpret because of its globular conformation unlike typical 'estradiol like' ligands that retain a planar substructure. Nevertheless, the previously defined filter could help in making choices between agonist and antagonist candidates upon docking poses.

The best combination of scores (MolDock, Rerank scores) occurs for receptors co-crystallized with agonist ligands, represented by canonical structures 1G50 and 2P15. In these cases, ferutinin showed the highest values of *Hit* descriptor. As illustrated in Figure 3A, the binding cavity of these structures was closed around 'estradiol like' ligands and ferutinin. These molecules along with ferutinin were able to place their phenol group in the same orientation inside the binding site in order to satisfy the hydrogen bonding network with ARG and GLU residues, and even with PHE404.

In the case of antagonist ligands in IXPC, 3ERT, and 2IOG structures, the binding cavity was extended in the β-face of the site to display a channel (C-cavity) explored by larger molecules (i.e., T-shaped) than estradiol. When ferutinin poses tend to benefit from this channel, they lose their conformity descriptors (CPC particularly) which generates fluctuations of Rerank score. A typical example was given by 1XPC as shown in Figure 3B.

Regarding ERβ canonical structures (Table 4), the worst CPC descriptor and Rerank score fluctuation were obtained with 1U3S and 1QKN structures even if the CBP descriptor was the best (conformity in the placement of the phenol group).Interestingly, best *Hit* values were obtained with 2IOJ (Chain C) and 1X7R structures.

According to these calculations, ferutinin was able to dock in opened or closed binding cavity of ERβ. Hence, conformation similarities (ester group and daucane core) were noticed between the four poses: 2IOJ (agonist), 1X7R (antagonist/agonist) for ERβ receptors and 2P15 (agonist), 2IOG (antagonist) for ERα receptors.

These results demonstrated that ferutinin could mimic the binding mode of estradiol in the α-face cavity with good scores (2YJA, 1G50) in both ERα and ERβ. Therefore, ferutinin was considered as an agonist for these receptors. However, in ERα, this compound was unable to fit into antagonists binding sites, exhibiting bad scores (3ERT). Based on these theoretical results, ferutinin could act preferentially as an agonist ligand of ERα. In the case of ERβ, ferutinin could act as an agonist (2YJA, 2IOJ). However, when this compound is docked into the binding site of 1X7R, it fits the C-cavity by means of its ester bond. Therefore, ferutinin could be considered as an antagonist to ERβ as well. Finally, on a structural basis, results issued from this docking filter indicate that ferutinin could be classified as an agonist to ERα and as an agonist/antagonist to ERβ while compound **3c'** could interact preferentially with both ER subtype as an antagonist.

Table 4: Docking scores of ferutinin in ERβ sites

Receptor	Canonical	Ligand class	MolDock score	Rerank score	CPC	CBP	Hit
ERβ	1QKN	Antagonist	20.22	611.41	3	+	
	1X7R	Agonist/antagonist	−134.22	−92.26	9	+	High
	2YJA	Agonist	−118.45	−19.07	8	+	
	2IOJ (C)	Agonist	−128.57	−81.96	9	+	High
	1U3S (A)	Agonist	−101.26	71.13	3	+	

Docking scores (arbitrary units) obtained using Molegro Virtual Docker after postdocking minimization. Ligand classes column: 2YJA, 2IOJ (C), 1U3S (A) structures are liganded with agonists, and 1QKN, 1X7R structures are liganded with mostly antagonists.

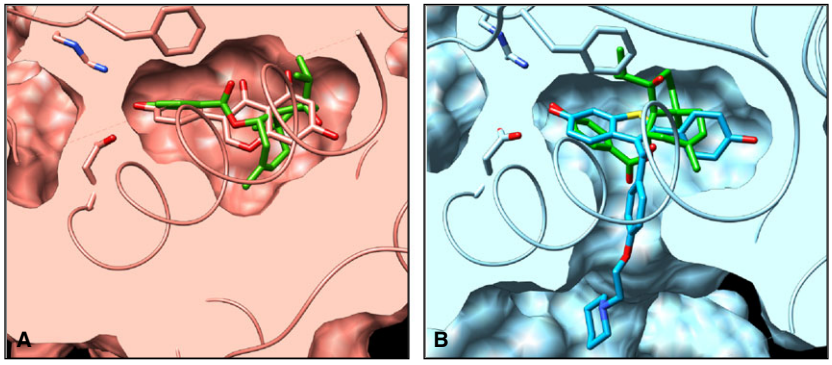

Figure 4: Docking poses of Ferutinin in ERβ binding cavities. Ferutinin (FRT, green) docking poses from Table 4 are shown in 1QKN (A, chain A, ERβ, cyan, opened cavity) and 1X7R (B, chain A, ERβ, salmon, closed cavity) structures, including the corresponding co-crystallized ligands RAL (blue, antagonist) and GEN (salmon, antagonist/agonist). The clipping planes of aligned structures are the same, and set using lateral chains of GLU 353 (1QKN:260) and ARG394 (1QKN: 301), PHE 404 (1QKN: 311) is also shown (left-up).

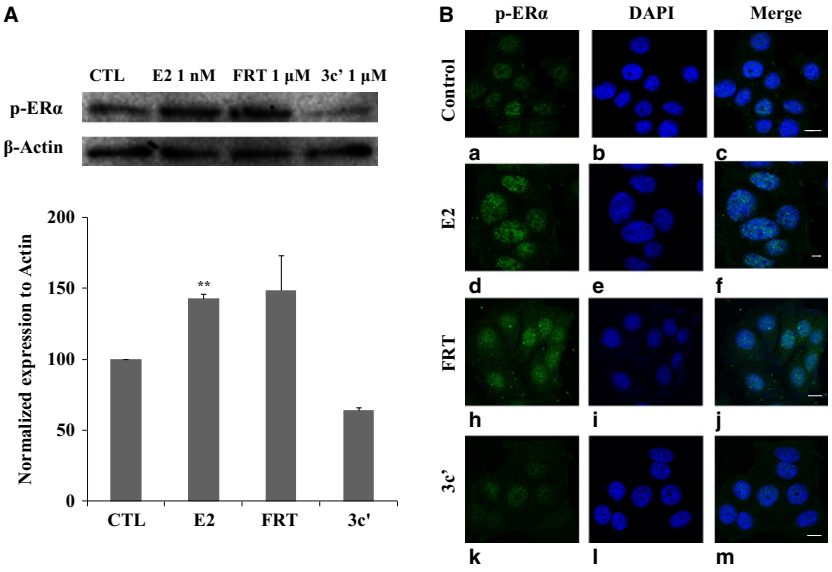

Figure 5: The effect of ferutinin and its potent analogue **3c'** on p-ERα protein levels and localization. (A) Phosphorylated Serine-118 ERα protein expression in MCF-7 cells treated with 1 nM estradiol (**E2**), 1 μM ferutinin (**FRT**), and 1 μM analogue (**3c'**) for 1 h. β-Actin was used as an internal control. The quantification of p-ERα levels is represented as percent increase or decrease compared to control levels and was evaluated in three independent experiments. The results were presented as the mean ± SEM. * and ** correspond to $p < 0.05$, and $p < 0.01$, respectively, versus the control group. (B) Immunostaining assay of p-ERα in MCF-7-treated cells with 1 nM E2, 1 μM FRT, and 1 μM 3c'. Scale bar (A → M) 5 μm.

Nevertheless, the interpretation of 4D docking data remains a complicated task when it comes to setting up the postdocking descriptors and the conformational sampling. At this level, an increase in the number of descriptors as well as sampling conformations could enhance the predictability of the calculation approach.

Molecular target ERα

The aforementioned results strongly suggested that ferutinin and its analogue **3c'** are ER ligands harboring an agonist and an antagonist activity, respectively. This hypothesis was examined directly by assessing p-ERα protein levels of MCF-7-treated cells using Western blot analysis. The phosphorylation of ERα is an early event in the activation of the signaling pathways inducing MCF-7 cell proliferation.

Ferutinin markedly increased p-ERα protein levels at low concentrations (1 μM), whereas compound **3c'** inhibited about 30% the phosphorylation of ERα when compared to the control non-treated cells (Figure 5A). The variation of ERα expression occurred as early as 1 h postferutinin treatment. As the phosphorylation of cytoplasmic ERα induces its translocation into the nucleus to activate the transcription machinery, we next examined the effect of ferutinin and its analogue on p-ERα localization. Immunostaining assay was performed on ferutinin and **3c'-**treated MCF-7 cells at low (1 μM).

Prior to 1 μM ferutinin treatment, the signal of p-ERα pool was more pronounced in the nucleus as compared to the control. The intensity of the signal in ferutinin treated cells is similar to 1 nM estradiol stimulation. However, a more diffuse cytoplasmic staining was seen when treating MCF-7 cells with the analogue **3c'** (Figure 5B). The acute change of ERα expression pattern is likely to be important in a myriad of differential cellular responses between ferutinin and its analogue.

The present findings demonstrate that compound **3c'** specifically suppress breast cancer cell proliferation by targeting ERα protein. These data are important to the mechanisms underlying the rapid anticancer effects of ferutinin and its analogue on MCF-7 estrogen-responsive cells. Nevertheless, the investigation on additional signaling pathways may help to elucidate the complete cytotoxic-inducing mechanism observed *in vitro*.

Conclusion

In this work, three series of ferutinin analogues were described and evaluated for their anticancer activity. The analogue **3c'** displayed significant and selective antiproliferative activity against the estrogen-dependent breast cancer cell line, MCF-7. Furthermore, molecular docking and functional assay showed that **3c'** binds as an antagonist to the ERα protein while ferutinin acts as an agonist. Compound **3c'**, being 10-folds more efficient than the currently used tamoxifen, could serve as a lead for further development of more potent drugs.

Acknowledgments

We would like to thanks AUF (Agence Universitaire de la Francophonie) for the financial support of the PhD student Remi Safi.

Conflict of Interest

All authors declare that they have no conflict of interest.

References

1. Anderson L.N., Cotterchio M., Boucher B.A., Kreiger N. (2013) Phytoestrogen intake from foods, during adolescence and adulthood, and risk of breast cancer by estrogen and progesterone receptor tumor subgroup among Ontario women. Int J Cancer;132:1683–1692.
2. Swann R., Perkins K.A., Velentzis L.S., Ciria C., Dutton S.J., Mulligan A.A., Woodside J.V., Cantwell M.M., Leathem A.J., Robertson C.E., Dwek M.V. (2013) The DietCompLyf study: a prospective cohort study of breast cancer survival and phytoestrogen consumption. Maturitas;75:232–240.
3. Iranshahi M., Arfa P., Ramezani M., Jaafari M.R., Sadeghian H., Bassarello C., Piacente S., Pizza C. (2007) New sesquiterpene coumarin from the roots of Ferula latisecta. Phytochemistry;68:554–561.
4. Iranshahi M., Kalategi F., Rezaee R., Shahverdi A.R., Ito C., Furukawa H., Tokuda H., Itoigawa M. (2008) Cancer chemopreventive activity of terpenoid coumarins from Ferula species. Planta Med;74:147–150.
5. Diab Y., Dolmazon R., Bessiere J.M. (2001) Daucane aryl esters composition from the Lebanese *Ferula hermonis* Boiss. (zallooh root). Flavour Fragr J;16:120–122.
6. Geroushi A., Auzi A.A., Elhwuegi A.S., Elzawam F., Elsherif A., Nahar L., Sarker S.D. (2011) Antiinflammatory sesquiterpenes from the root oil of *Ferula hermonis*. Phytother Res;25:774–777.
7. Hadidi K.A., Aburjai T., Battah A.K. (2003) A comparative study of Ferula hermonis root extracts and sildenafil on copulatory behaviour of male rats. Fitoterapia;74:242–246.
8. Hilan C., Sfeir R., El Hage R., Jawich D., Frem M.E., Jawhar K. (2007) Chimiotypes de plantes communes au Liban du genre Origanum et du genre Micromeria (Lamiceae). Lebanese Sci J;8:135–151.
9. Palumbo C., Ferretti M., Bertoni L., Cavani F., Resca E., Casolari B., Carnevale G., Zavatti M., Montanari C., Benelli A., Zanoli P.J. (2009) Influence of ferutinin on bone metabolism in ovariectomized rats. I: role in preventing osteoporosis. Bone Miner Metab;27:538–545.
10. Ferretti M., Bertoni L., Cavani F., Zavatti M., Resca E., Carnevale G., Benelli A., Zanoli P., Palumbo C.J. (2010) Influence of ferutinin on bone metabolism in ovariectomized rats. II: role in recovering osteoporosis. J Anat;217:48–56.
11. Macho A., Blanco-Molina M., Spagliardi P., Appendino G., Bremner P., Heinrich M., Fiebich B.L., Munoz E. (2004) Calcium ionophoretic and apoptotic effects of ferutinin in the human Jurkat T-cell line. Pharmacol;68:875–883.
12. Ikeda K., Arao Y., Otsuka H., Nomoto S., Horiguchi H., Kato S., Kayama F. (2002) Terpenoids found in the *Umbelliferae* family act as agonists/antagonists for ER(alpha) and ER(beta): differential transcription activity between ferutinine-liganded ER(alpha) and ER(beta). Biochem Biophys Res Commun;291:354–360.
13. Appendino G., Spagliardi P., Cravotto G., Pocock V., Milligan S.J. (2002) Daucane phytoestrogens: a structure-activity study. J Nat Prod;65:1612–1615.
14. Lhuiler A., Fabre N., Cheble E., Oueida F., Maurel S., Valentin A., Fouraste I., Moulis C. (2005) Daucane sesquiterpenes from *Ferula hermonis*. J Nat Prod;68:468–471.
15. Kuete V., Wiench B., Hegazy M.E.F., Mohamed T.A., Fankam A.G., Shahat A.A., Efferth T. (2012) Antibacterial activity and cytotoxicity from selected Egyptians medicinal plants. Planta Med;78:193–199.
16. Dall'Acqua S., Linardi M.A., Maggi F., Nicoletti M., Petitto V., Innocenti G., Basso G., Viola G. (2011) Natural daucane sesquiterpenes with antiproliferative and proapoptotic activity against human tumor cells. Bioorg Med Chem;19:5876–5885.
17. Poli F., Appendino G., Sacchetti G., Ballero M., Maggiano N., Ranelletti F.O. (2005) Antiproliferative effects of daucane esters from *Ferula communis* and *F. arrigonii* on human colon cancer cell lines. Phytother Res;19:152–157.
18. Pettersen E.F., Goddard T.D., Huang C.C., Couch G.S., Greenblatt D.M., Meng E.C., Ferrin T.E. (2004) UCSF Chimera—A visualization system for exploratory research and analysis. J Comput Chem;25:1605–1612.
19. Meng E.C., Pettersen E.F., Couch G.S., Huang C.C., Ferrin T.E. (2006) Tools for integrated sequence-structure analysis with UCSF chimera. BMC Bioinformatics;7:339–349.
20. Thomsen R., Christensen M. (2006) MolDock: a new technique for high accuracy molecular docking. J Med Chem;49:3315–3321.
21. Bombarrdelli E., Cairoli G., Fontana G., Cristoni A., Mercalli E. (2008) US Patent 7, 371, 886 B2.
22. Nadelson J., Simpson R.J., Anderson R.C., Bajwa J.S. (1995) US Patent 5, 378, 728.
23. Appendino G., Spagliardi P., Sterner O., Milligan S.J. (2004) Structure-activity relationships of the estrogenic sesquiterpene ester ferutinin. Modification of the terpenoid core. J Nat Prod;67:1557–1564.
24. LeBlanc M.L., Paré A.F., Jean-François J., Hébert M.J.G., Surette M.E., Touaibia M. (2012) Synthesis and antiradical/antioxidant activities of caffeic acid phenethyl ester and its related propionic, acetic, and benzoic acid analogues. Molecules;17:14637–14650.
25. So-Jung Park S.J., Kufareva I., Abagyan R. (2010) Improved docking, screening and selectivity prediction for small molecule nuclear receptor modulators using conformational ensembles. J Comput Aided Mol Des;24:459–471.
26. Prouillac C., Koraichi F., Videmann B., Mazallon M., Rodriguez F., Baltas M., Lecoeur S. (2012) In vitro

toxicological effects of estrogenic mycotoxins on human placental cells: structure activity relationships. Toxicol Appl Pharmacol;259:366–375.
27. Bottegoni G., Kufareva I., Totrov M., Abagyan R. (2009) Four-dimensional docking: a fast and accurate account of discrete receptor flexibility in ligand docking. J Med Chem;52:397–406.
28. Sousa S.F., Ribeiro A.J.M., Coimbra J.T.S., Neves R.P.P., Martins S.A., Moorthy N.S.H.N., Fernandes P.A., Ramos M. (2013) Protein-ligand docking in the new millennium-a retrospective of 10 years in the field. Curr Med Chem;20:2296–2314.

Supporting Information

Additional Supporting Information may be found in the online version of this article:

Appendix S1. Definition of canonical sets (ERα, ERβ) for receptors' structures.

Table S1. Structural classification of ERα liganded structures.

Table S2. Structural classification of ERβ liganded structures.